

Status of experimental and evaluated cross sections for the  $^{209}\text{Bi}(n,3n)^{207}\text{Bi}$  reactions.

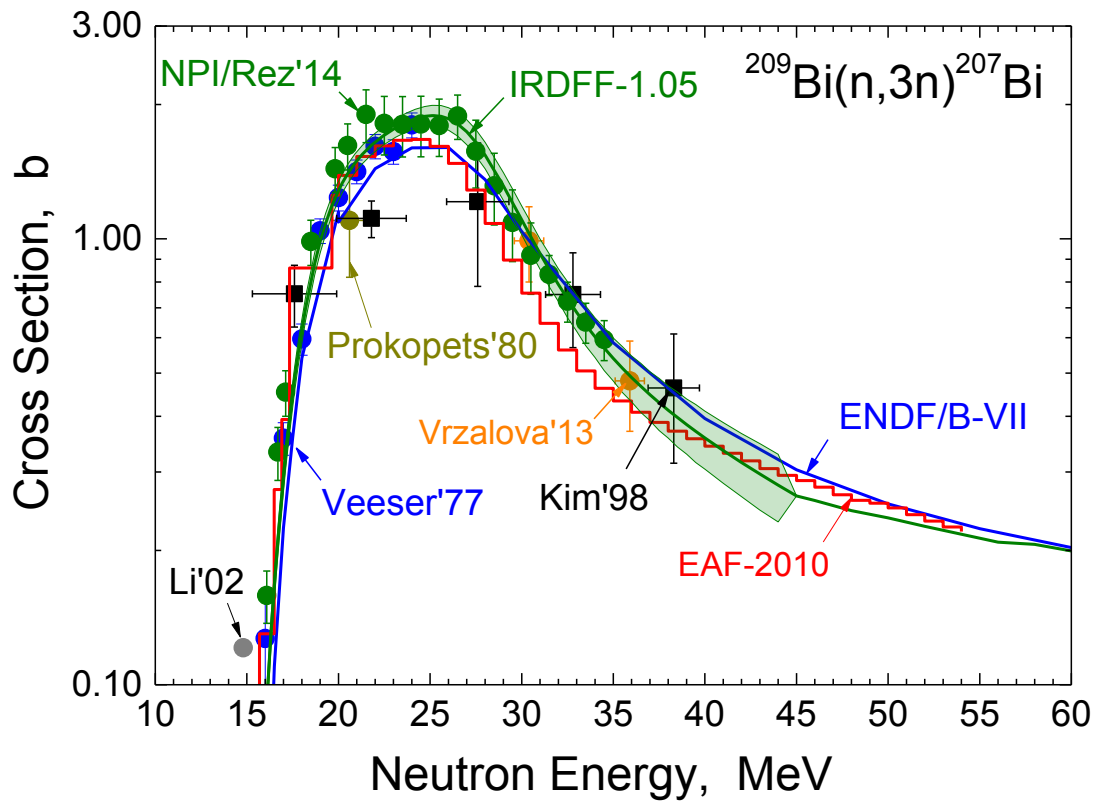


Fig. 1. Experimental and Evaluated data for the  $^{209}\text{Bi}(n,3n)^{207}\text{Bi}$  cross section.

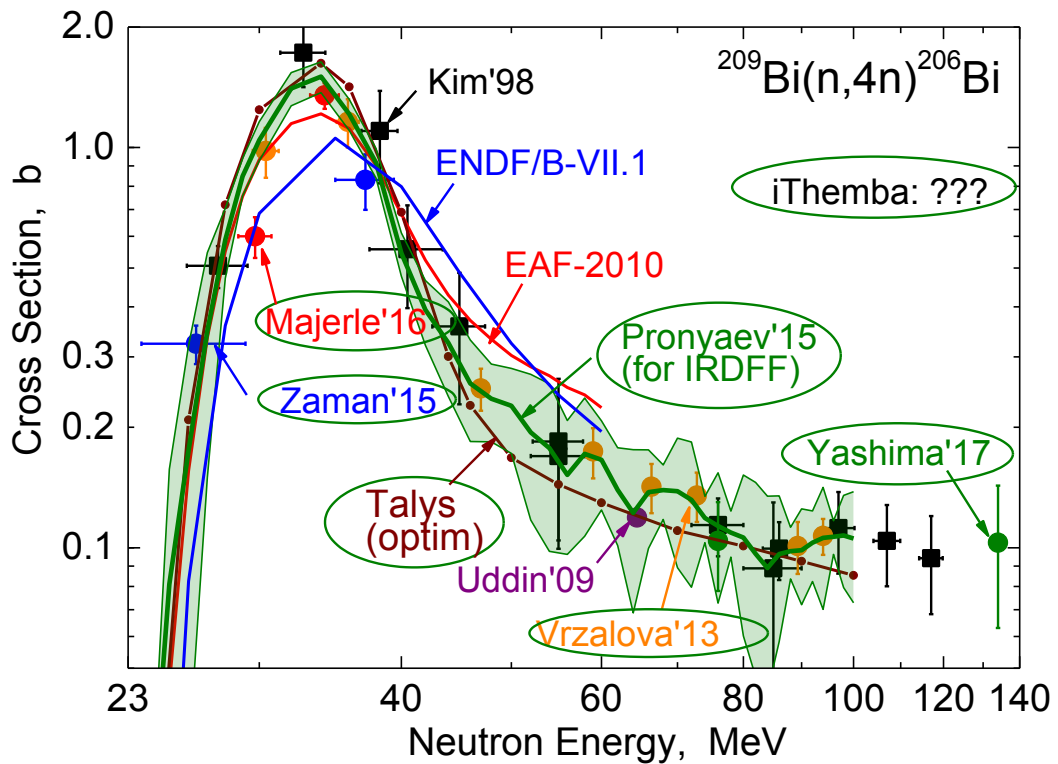


Fig. 2. Experimental and Evaluated data for the  $^{209}\text{Bi}(n,4n)^{206}\text{Bi}$  cross section.

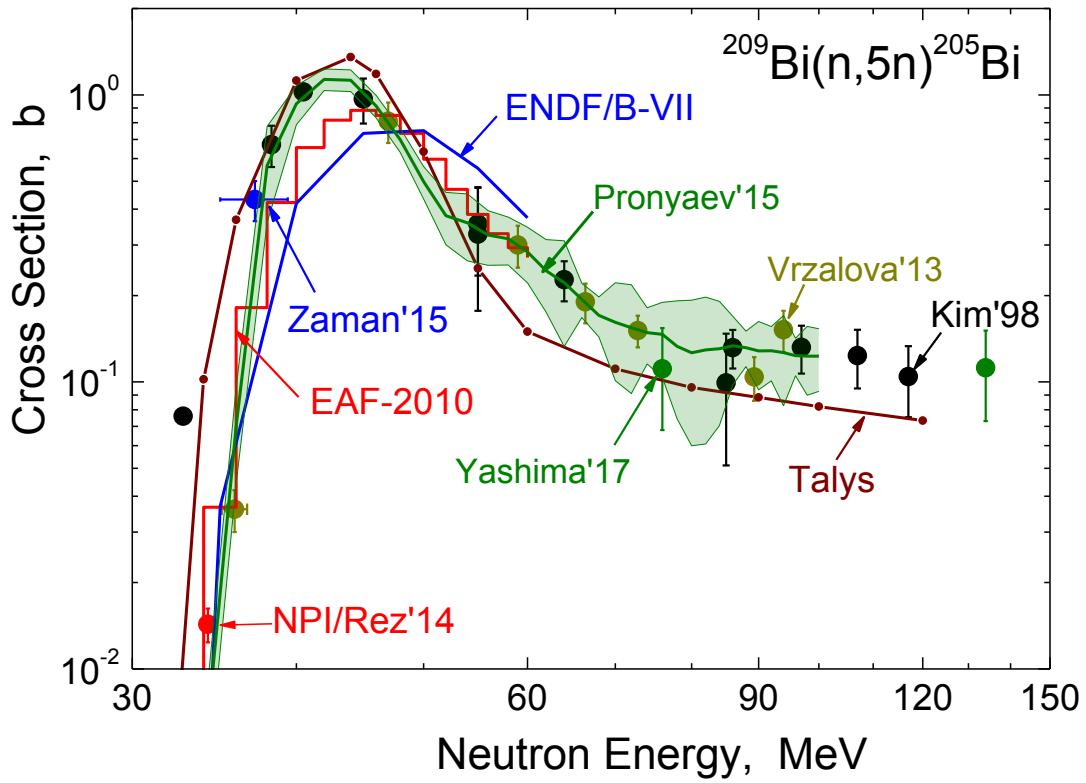


Fig. 3. Experimental and Evaluated data for the  $^{209}\text{Bi}(n,5n)^{205}\text{Bi}$  cross section.

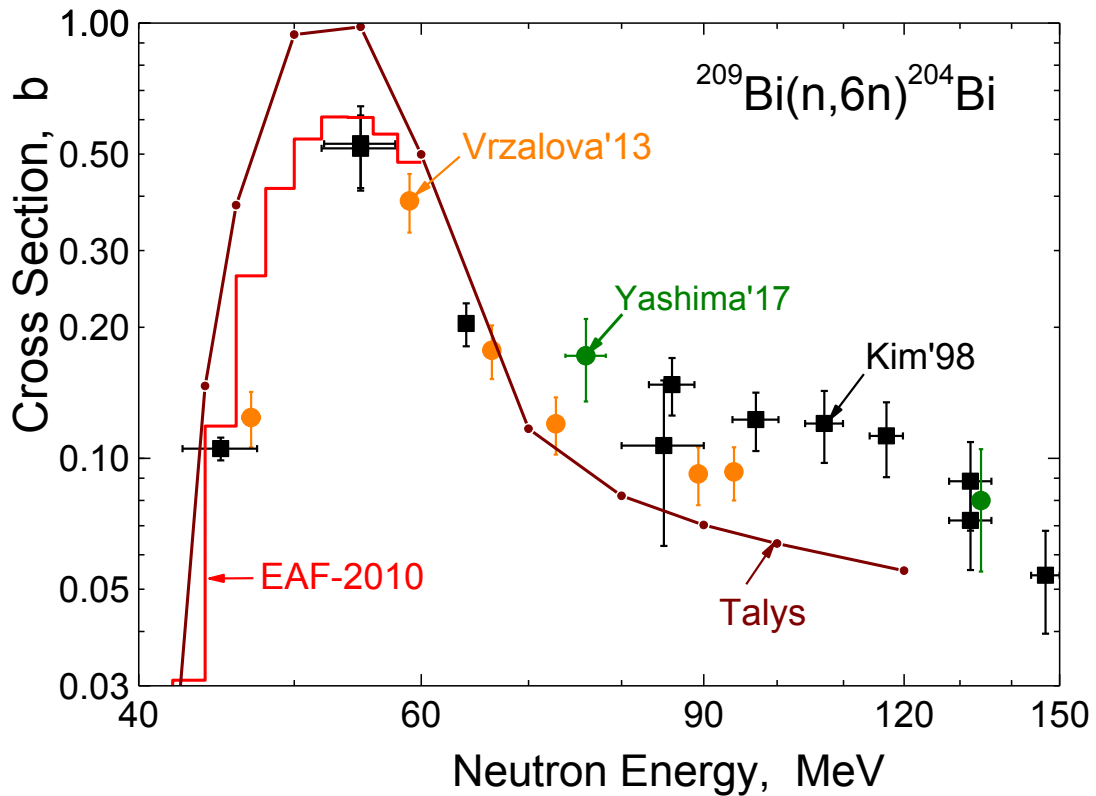


Fig. 4. Experimental and Evaluated data for the  $^{209}\text{Bi}(n,6n)^{204}\text{Bi}$  cross section.

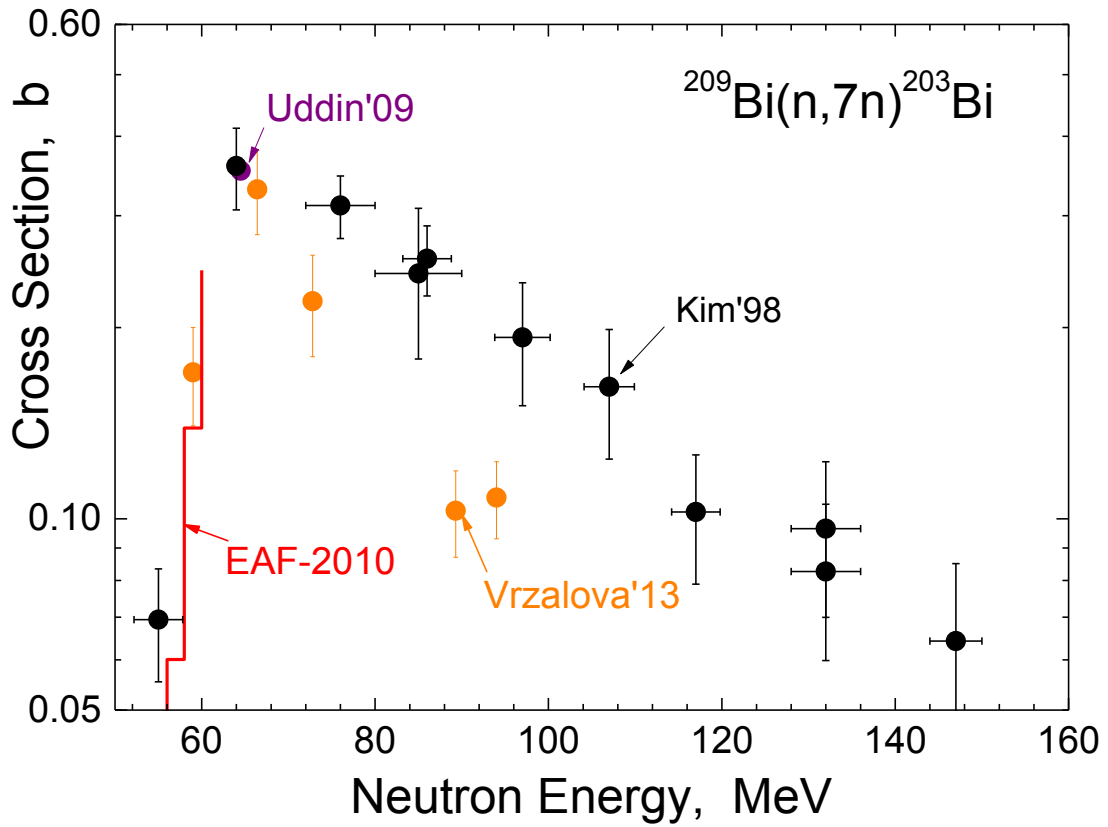


Fig. 5. Experimental and Evaluated data for the  $^{209}\text{Bi}(n,7n)^{203}\text{Bi}$  cross section.

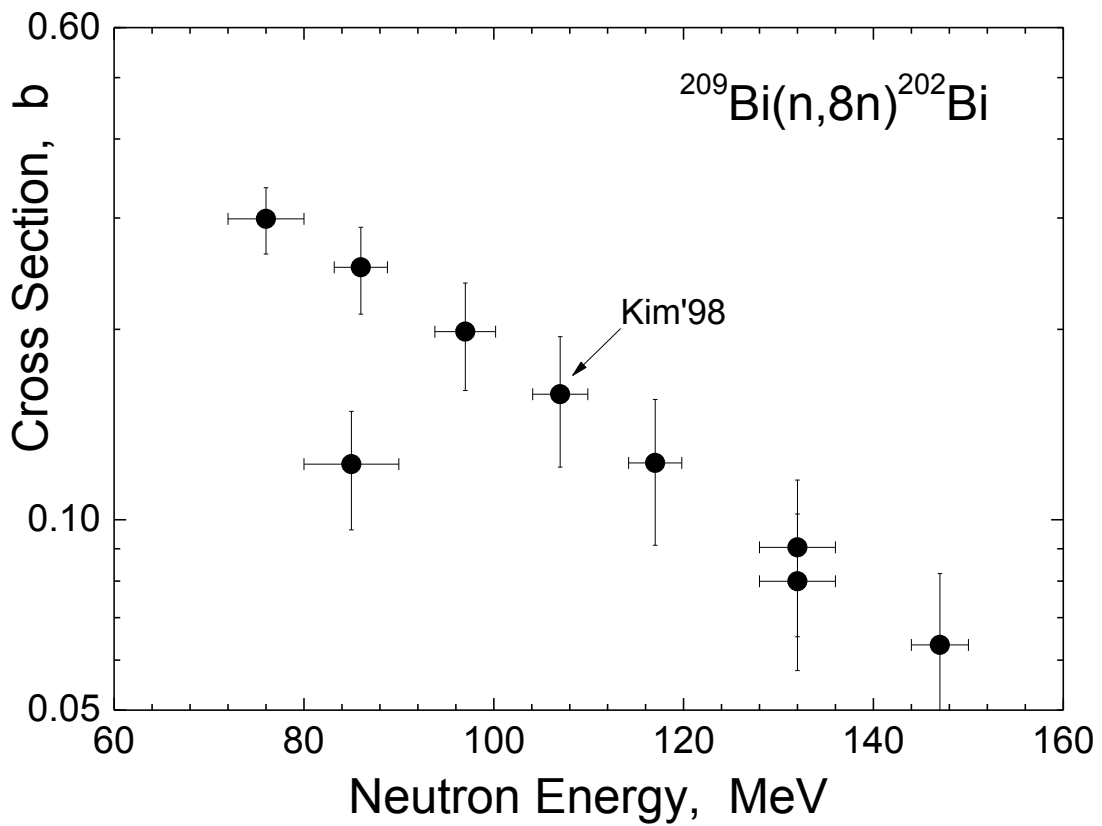


Fig. 6. Experimental and Evaluated data for the  $^{209}\text{Bi}(n,8n)^{202}\text{Bi}$  cross section.

# High-energy (n,xn) dosimetry reactions

V.G. Pronyaev (pronyaev@ippe.ru)  
IPPE, Obninsk, Russia

1. Most DOS reactions are used for spectra unfolding below 15 MeV (IRDF-2002)
2. They have rather “flat” shape in the energy range from 20 MeV to 100 MeV

# High-energy (n,xn) dosimetry reactions

## Requirements:

1. Bell- or step-wise shape of the cross sections (ideal – delta or step function)
2. Shifted on energy relative each other
3. Minimal number of dosimetry samples for unfolding with a few MeV resolution
4. High activation cross sections, half-lives convenient for measurements and high quantum gamma-yields
5. Gamma-line energies in the region of maximum of the detector efficiency
6. No, or minimal admixture from “parasitic” gamma-lines which can not be separated through energy resolution of detector or times of activation, cooling and activity measurement

# High-energy (n,xn) dosimetry reactions

## Best reactions for high energy dosimetry:

1.  $Z^N(n,xn)Z^{N-x-1}$  reactions
2. Natural mono-isotopic samples
3. Medium or heavy atomic weight – high non-elastic, high cross sections for neutron emission, low for charged particle emission
4.  $x=1, \dots, 10$  for heavy samples, reactions covering the energy below 100 MeV
5.  $x=1, \dots, 10$  for medium weight samples, have different thresholds relative thresholds in heavy samples

# High-energy (n,xn) dosimetry reactions

## Drawbacks of (n,xn) reactions:

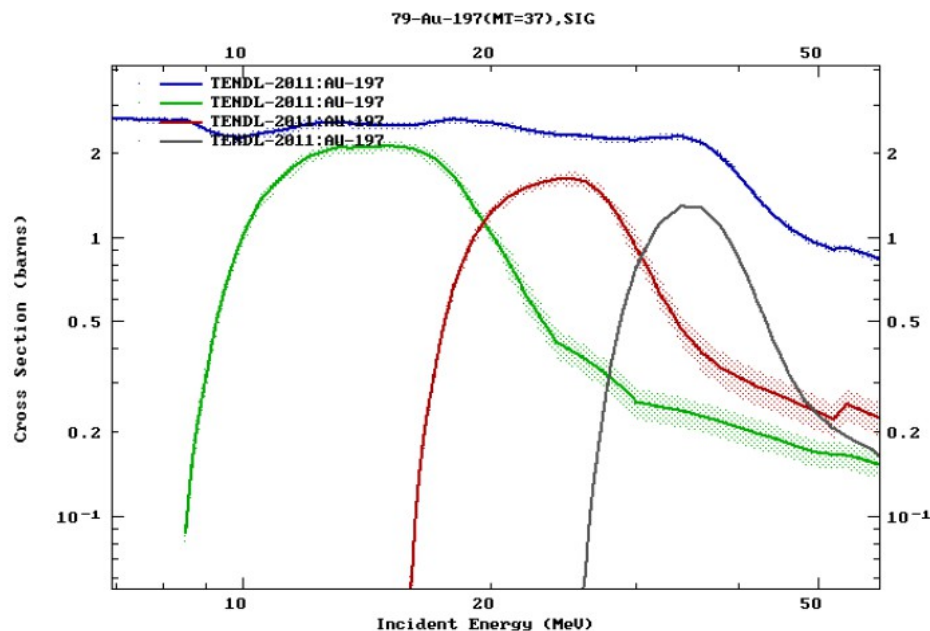
1. Energy resolution of unfolded spectrum can not be better than widths of bell-shaped form of the cross section (between 10 and 15 MeV) or difference between thresholds
2. Width of the bell is increasing with the  $x$
3. (n,xn) cross sections in the maximum are decreasing with  $x$  increasing
4. Bell-shape of cross section is converting in step-shape form with increasing of  $x$ . This is probably not a drawback

# High-energy (n,xn) dosimetry reactions

**Mono-isotopic samples which can be used:**

$^{209}\text{Bi}$ ,  $^{197}\text{Au}$ ,  $^{139}\text{La}$  (99.91%) and  $^{103}\text{Rh}$

**Example of cross sections for  $^{197}\text{Au}$ :**



TENDL-2011 library

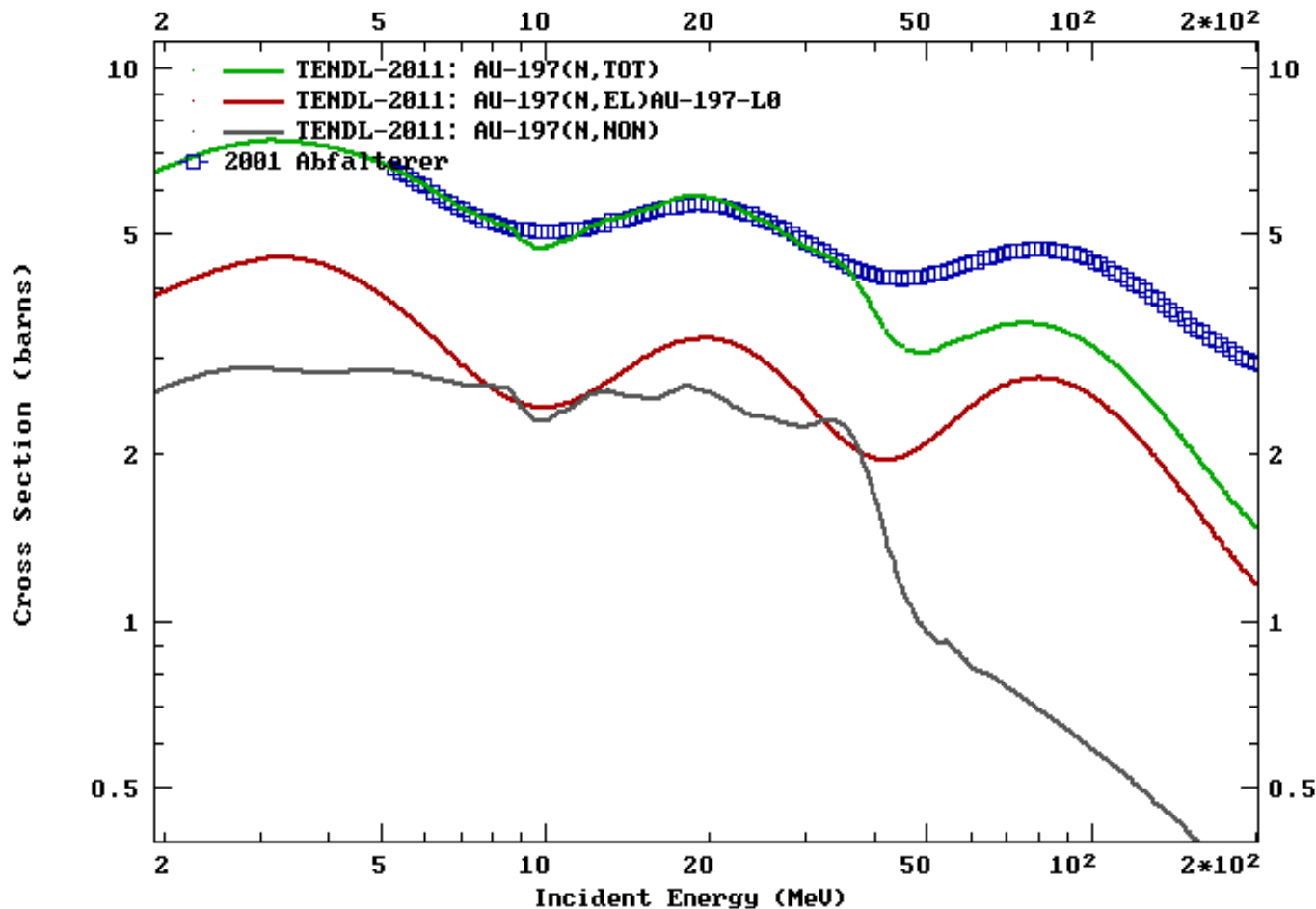
blue – non-elastic  
green – (n,2n)  
red – (n,3n)  
gray – (n,4n)

Above 33 MeV non-elastic (MT=3) is wrong in TENDL-2011 library



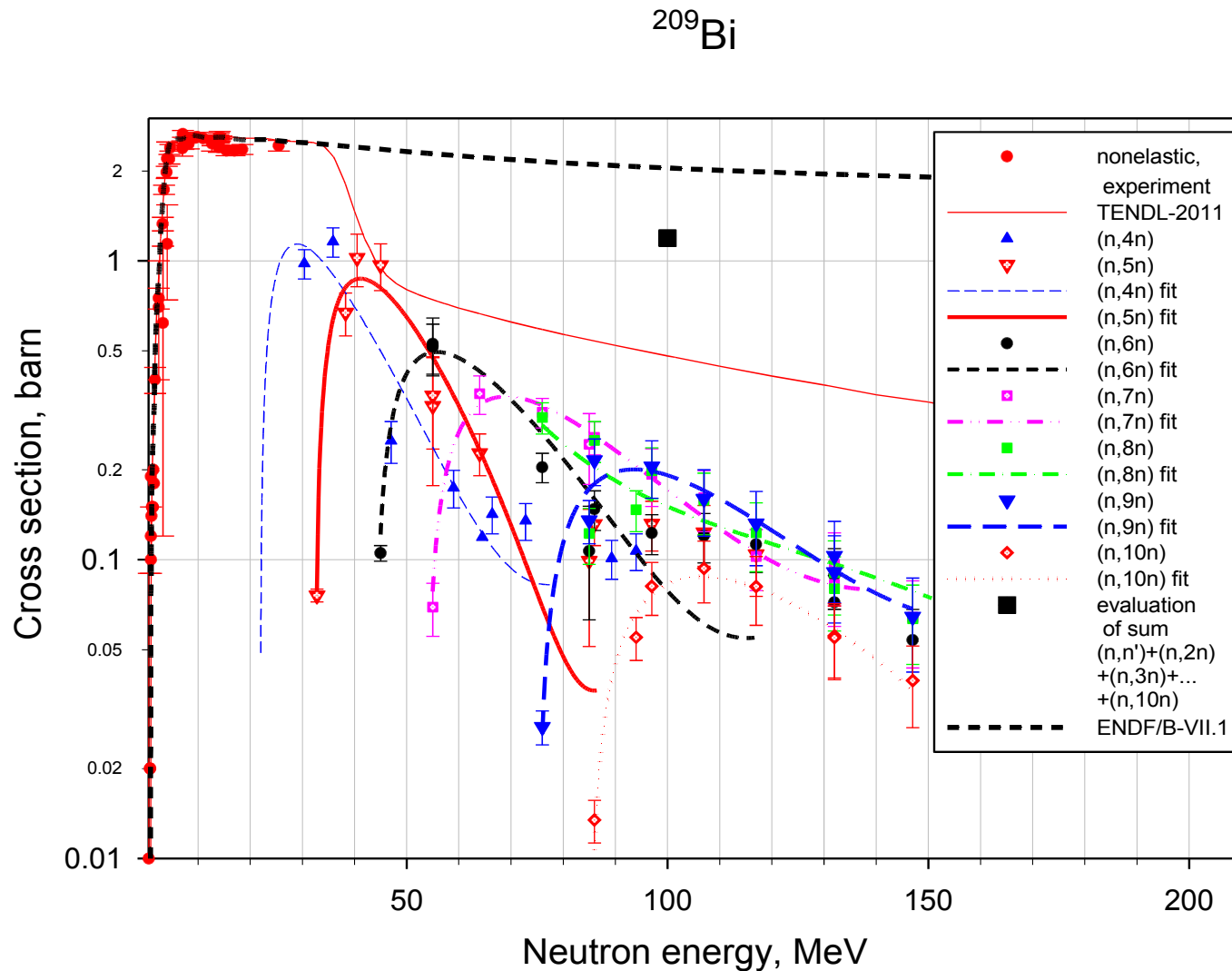
# High-energy (n,xn) dosimetry reactions

ENDF Request 1700, 2013-May-06,04:57:54  
EXFOR Request: 2061/1, 2013-May-06 04:58:46



TENDL-2011 library has wrong total cross section (green line) above 33 MeV because non-elastic (gray line) and all (n,xn) reactions for  $x > 4$  are wrongly given under MT=5. Experimental data for total cross section are high-accuracy data by Abfalterer et al.

# High-energy (n,xn) dosimetry reactions



Comparison of experimental data – **nonelastic** taken from EXFOR and **(n,xn)** by E. Kim, T. Nakamura, A. Konno et al. Nucl. Sci. Eng., 129, p.209 (1988) with TENDL-2011 and ENDF/B-VII.1 evaluation for non-elastic and inverse 3-rd order polynomial fit for (n,xn) reactions.

# High-energy (n,xn) dosimetry reactions

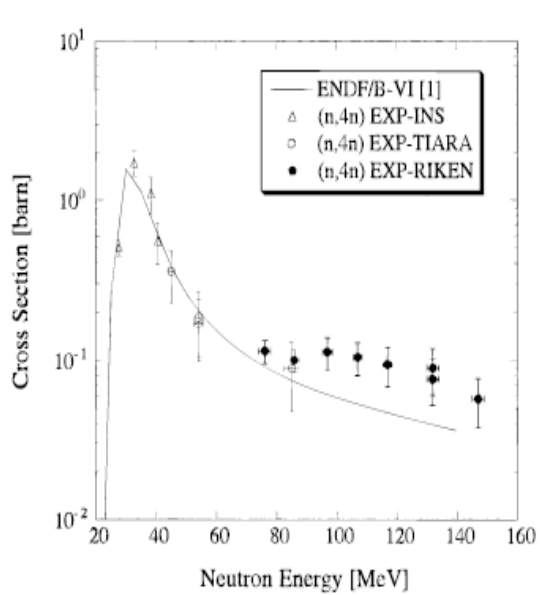


Fig. 9.  $^{209}\text{Bi}(n,4n)^{206}\text{Bi}$  reaction cross section.

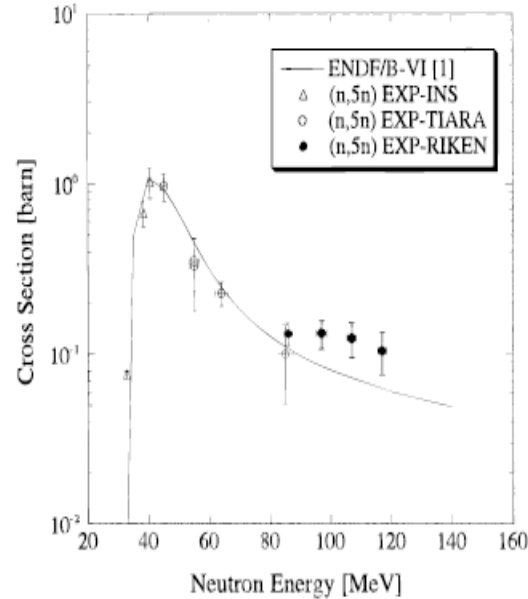


Fig. 10.  $^{209}\text{Bi}(n,5n)^{205}\text{Bi}$  reaction cross section.

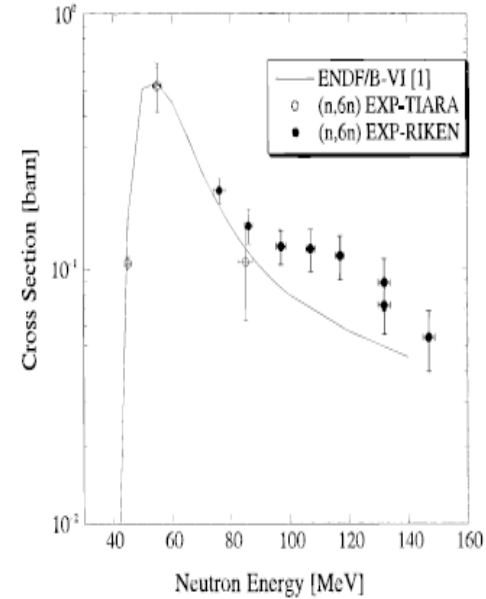


Fig. 11.  $^{209}\text{Bi}(n,6n)^{204}\text{Bi}$  reaction cross section.

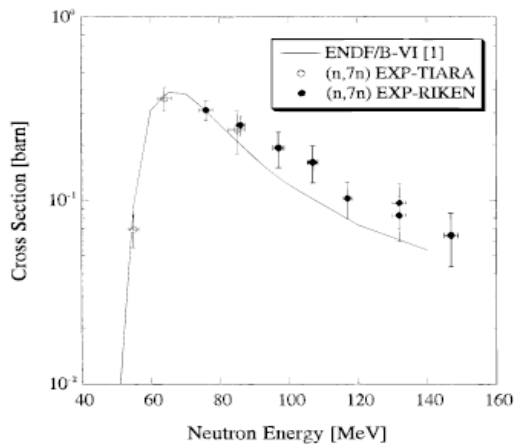


Fig. 12.  $^{209}\text{Bi}(n,7n)^{203}\text{Bi}$  reaction cross section.

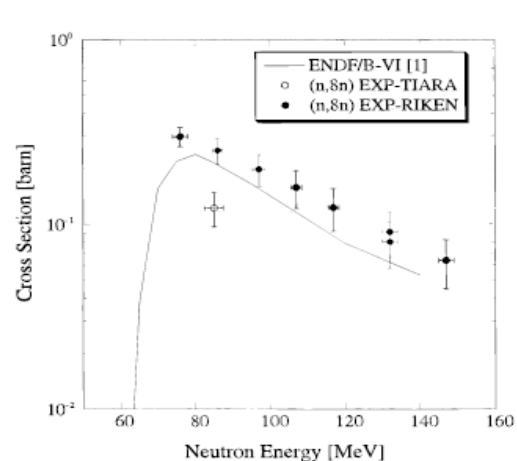


Fig. 13.  $^{209}\text{Bi}(n,8n)^{202}\text{Bi}$  reaction cross section.

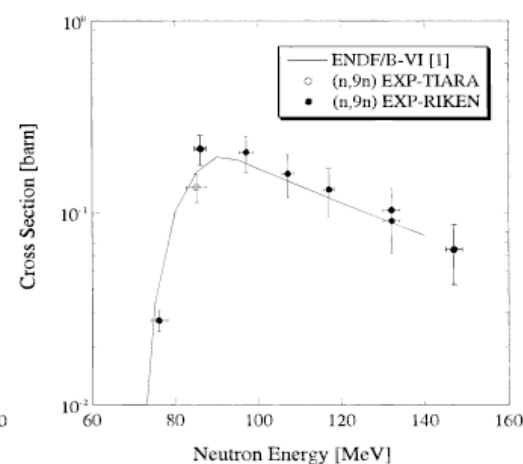


Fig. 14.  $^{209}\text{Bi}(n,9n)^{201}\text{Bi}$  reaction cross section.

**Comparison of (n,xn) experimental data by E. Kim, T. Nakamura, A. Konno et al. Nucl. Sci. Eng., 129, p.209 (1988) with ENDF/B-VI (=ENDF/B-VII.1) evaluation done independently from exp. data. Taken from publication by Kim et al..**

# Properties of (n,xn) CS and Residual Nuclei Decays for $^{197}\text{Au}(n,xn)$ and $^{209}\text{Bi}(n,xn)$

Target and reaction, ( $E_{\text{thresh}}$ , MeV)	Residual nucleus	Cross section MAX, b	Energy of MAX CS, MeV	Half-width of the MAX, MeV	Half-life of residual nucleus	$\gamma$ -lines after decay, keV	$\gamma$ -line yield, %	Parasitic gammas, $\pm 5$ keV for yields $>1\%$
$^{197}\text{Au}(n,2n)$ (8.114)	$^{196}\text{gAu}$	2.1	14.5	10	6.1669 d	355.73 333.03	87 22.9	7n, 353.88, 2.7 % , 3.18 h 5n, 328.5, 60.4 % , 38.02h
$^{197}\text{Au}(n,3n)$ (14.790)	$^{195}\text{gAu}$	2.0	26	11	180.098 d	98.88	11.2	not known
$^{197}\text{Au}(n,4n)$ (23.260)	$^{194}\text{gAu}$	1.4	32	10	38.02 h	328.464	60.4	2n, 333, 22.9%, 6.17 d
$^{209}\text{Bi}(n,4n)$ (22.553)	$^{206}\text{gBi}$	1.65	33	10	6.243 d	516.8 537.45 803.1 881.01	40.8 30.5 99.0 66.2	6n, 532.7, 1.36%, 11.32h 8n, 876.2, 1.06%, 1.71h 9n, 879.6, 1.8 % , 103 min
$^{209}\text{Bi}(n,5n)$ (29.622)	$^{205}\text{gBi}$	1.2	44	10	15.31 d	703.45 987.66 1764.3	31.1 16.1 32.5	6n, 983.98 59 % , 11,22 h
$^{209}\text{Bi}(n,6n)$ (38.152)	$^{204}\text{gBi}$	0.55	55	12	11.22 h	374.76 899.15 983.98	82.0 99.0 59.0	7n, 896.9, 13.2%, 11.76h 9n, 902.0, 9.0 % , 103 min 9n, 990.6, 3.51 % , 103 min
$^{209}\text{Bi}(n,7n)$ (45.380)	$^{203}\text{gBi}$	0.36	65	18	11.76 h	820.2 825.2 896.9	30.0 14.8 13.2	9n, 818.9, 8.0 % , 103 min 7n, 816.3, 4.1 % , 11.76 h 4n, 895.1, 15.67 % , 6.243 d 6n, 899.1, 99 % , 11,22 h
$^{209}\text{Bi}(n,8n)$ (54.277)	$^{202}\text{gBi}$	0.30	75	30	1.71 h	422.13 657.49 960.67	83.7 60.6 99.283	6n, 421.6, 1.14 % , 11.22h 10n, 419.77, 91 % , 36.4 m 4n, 657.2 1.91 % , 6.243 d 6n, 661.58, 2.6 % , 11.22 h
$^{209}\text{Bi}(n,9n)$ (61.710)	$^{201}\text{gBi}$	0.22	87	40	1.717 h	629.1 936.2 1014.	26.0 12.2 11.6	7n, 633.8, 1.3 % , 11.76 h 4n, 632.25, 4.47 % , 6.243 d 7n, 933.4, 1.5 % , 11.76 h 10n, 931.7 5, 2.6 % , 36.4 m 935.3, 1.4 % , 36.4 m 4n, 1018.6, 7.60 % , 6.243 d
$^{209}\text{Bi}(n,10n)$	$^{200}\text{gBi}$	0.10	100	50	36.4 m	1026.5	100	not known

# Properties of (n,xn) CS and Residual Nuclei Decays for $^{139}\text{La}(n,xn)$ and $^{103}\text{Rh}(n,xn)$

Target and reaction, ( $E_{\text{thresh}}$ , MeV)	Residual nucleus	Max. cross section, b	Energy where CS has a maximum MeV	Half-width of the maximum MeV	Half-life of residual nucleus	Gamma-lines after decay, keV	Gamma-line quantum yield, %	Parasitic gammas, $\pm 5$ keV for yields $>1\%$
$^{139}\text{La}(n,4n)$ (25.590)	$^{136g}\text{La}$	1.02	38	16	9.87 m	818.51	2.3	not known
$^{139}\text{La}(n,5n)$ (33.109)	$^{135g}\text{La}$				19.5 h	480.5	1.52	8n, 479.47, 3.5%
$^{139}\text{La}(n,6n)$ (42.674)	$^{134g}\text{La}$				6.45 m	604.7	5.04	8n, 601.75, 1.5%
$^{139}\text{La}(n,7n)$ (50.526)	$^{133g}\text{La}$				3.912 h	278.735	2.44	not known
$^{139}\text{La}(n,8n)$ (60.440)	$^{132g}\text{La}$ $^{132m}\text{La}$				24.3 m 4.8 h	464.55 663.7 464.55	21.6 11.2 76%	not known not known not known
$^{139}\text{La}(n,9n)$ (68.524)	$^{131g}\text{La}$				59.0 m	108.08 285.2 365.16 417.783	25.0 12.4 16.9 18.0	not known 9n, 285.4, 24% 7n, 290.6, 1.38% not known
$^{139}\text{La}(n,10n)$ (38.099)	$^{130g}\text{La}$				8.7 m	357.4 544.5 550.7	81. 16.2 25.9	not known 8n, 540.36, 7.7% 6n, 541.2, 39.2% not known
$^{103}\text{Rh}(n,4n)$ (26.915)	$^{100g}\text{Rh}$	0.5	40	20	20.8 h	539.5 822.7	80.6 21.1	not known not known
$^{103}\text{Rh}(n,5n)$ (35.076)	$^{99g}\text{Rh}$ $^{99m}\text{Rh}$				16.1 d 4.7 h	353.05 340.8	34.6 69.	not known not known
$^{103}\text{Rh}(n,6n)$ (45.653)	$^{98g}\text{Rh}$ $^{98m}\text{Rh}$				8.72 m 3.6 m	652.6 IT	97. 89.	not known
$^{103}\text{Rh}(n,7n)$ (54.388)	$^{97g}\text{Rh}$ $^{97m}\text{Rh}$				30.7 m 46.2 m	421.55 189.21	74.63 48.5	not known not known
$^{103}\text{Rh}(n,8n)$ (65.476)	$^{96g}\text{Rh}$ $^{96m}\text{Rh}$				9.90 m 1.51 m	631.73 52.	74.5 60.	2n, 628.05, 4.5% not known

# Conclusion

1. Reactions  $(n, xn)$  at natural mono-isotopic targets are good candidates for use in the neutron dosimetry for spectra in the energy range between 15 and 100 MeV
2. Gamma-lines from decay of different residual nuclei can be separated not only through energy resolution of the detectors but also through choosing of optimal irradiation, cooling and measurement times
3. Although the energy resolution for the unfolded spectra in case of use of one mono-isotopic detector is low (between 8 – 15 MeV), it can be improved if some set of natural mono-isotopic targets (with shifted thresholds for  $(n, 3n)$ ,  $(n, 4n)$ , ... reactions) will be used
4. New precision measurements, calculations and measurement are needed to achieve the accuracy needed for the use of these reactions for dosimetry purposes
5. The extension of energy range of the reactions used in the reactor dosimetry to high energies is not productive for use in high energy dosimetry because the most cross sections are rather flat at these energies